

METHODS OF CRYOSPHERE STUDIES

SATELLITE REMOTE SENSING ESTIMATION OF THAW LAKE AREAS:
ACCURACY ASSESSMENT

S.G. Kornienko

Oil and Gas Research Institute, RAS, 3 Gubkin str., Moscow, 119333, Russia; spaceakm2@ogri.ru

The accuracy of inland water body areas estimated from *GeoEye-1* and *Landsat 5* multiband satellite remote sensing data of different spatial resolutions is assessed with reference to examples of thaw lakes upon permafrost in the western coast of the Yamal Peninsula (Marre-Sale district). The surface area accuracy in the case of classification of water bodies depends on the selected number of land cover types (classes). The errors correlate with lake area and spatial resolution, for which the respective empirical relationships have been obtained.

Thaw lake, water body area, measurement error, satellite remote sensing, spatial resolution

INTRODUCTION

Prompt response to geological and permafrost hazards is an important prerequisite of environmental and production safety in the course of Arctic and Subarctic development. The state and dynamics of permafrost can be judged from the behavior of inland water bodies, especially thermokarst or thaw lakes. The surficial areal extent of these lakes often fluctuates as a result of man-caused or natural (weather and climate or tectonic) processes, and thus becomes a proxy of hazardous effects, provided that it is estimated to a sufficient accuracy.

Different features of thaw lakes, including the variability of their surface areas, are commonly studied by satellite remote sensing [Frohn *et al.*, 2005; Bryksina and Polishchuk, 2009; Dneprovskaya *et al.*, 2009; Kravtsova and Bystrova, 2009; Elsakov and Marushchak, 2011; Kravtsova and Tarasenko, 2011; Baranov *et al.*, 2012; Chen *et al.*, 2013]. Satellite imagery furnishes valuable information for analysis and prediction of global, regional, and local natural and anthropogenic effects in high latitudes. However, the lake area accuracy has received little attention so far, which makes it difficult to estimate the relevant changes.

Since the issue has been rarely in focus, it is hard to synthesize the available knowledge, to compare data, and to elaborate recommendations or norms for further scientific and practical applications. The few studies on the point include, for example, papers by Bryksina and Polishchuk [2013] or Chirico and Malpeli [2012], which however overlook some methodological aspects of remote sensing quantification of lake areas and the accuracy controls. No empirical re-

lationships have been suggested to correlate errors with lake areas and with the spatial resolution of satellite imagery. Solving these problems will allow higher-quality monitoring of variations in thaw lakes or other basins as indicators of permafrost changes. In this study the accuracy of inland water body areas estimated from *GeoEye-1* and *Landsat 5* multiband satellite remote sensing data of different spatial resolutions is assessed with reference to examples of thaw lakes upon permafrost in the western coast of the Yamal Peninsula (Marre-Sale district).

ERRORS IN LAKE AREA ESTIMATES
FROM SATELLITE IMAGERY

The accuracy of lake areas estimated by satellite imagery remote sensing depends on the properties of the target water body (its surface area, geometry or shoreline curvature, and water clarity), performance of the sensing system (resolution, bands, angle), acquisition conditions (illumination and state of the atmosphere), and data processing (classification algorithms, band combinations, etc.). Other things being equal, the accuracy decreases as the surface area of water bodies decreases and the shoreline curvature increases [Bryksina and Polishchuk, 2013]. The geometry of water bodies is better resolvable within the infrared bandwidth [Kondratiev and Shumakov, 1990], which is also used to estimate the relative water clarity to depths shallower than 2 m and the contents of chlorophyll *a* (>10 mg/l) and inorganic suspended matter (>10 mg/l) [Kondratiev and Shumakov, 1990]. Highly turbid shallow water can be misclassified as land, which worsens the accuracy of lake areas.

The lake areas are less accurate if the resolution of images is lower and the off-nadir angles are higher. The latter factor means that optical imagery provides a better quality of estimates than radar data, under otherwise equal conditions. However, the use of optical systems is limited by atmospheric conditions such as heavy cloud cover: even minor decrease in atmospheric transmission obscures water-land contrasts and, correspondingly, increases errors. Furthermore, the accuracy of optical data worsens at lower solar illumination angles. These factors are objective sources of error, which have to be taken into account in selection and analysis of data.

The accuracy of surface area estimates depends strongly on processing techniques, especially on the combination of spectral bands and algorithms for identification and classification of water bodies, i.e., the same spaceborne data processed with different methods may give more or less accurate results. Some known algorithms are: adaptive classification used for mapping thaw lakes from one-band near-infrared *Landsat 5* scenes [Kravtsova and Bystrova, 2009; Kravtsova and Tarasenko, 2011]; *Tasseled Cap* classification and mixed pixel decomposition [Elsakov and Marushchak, 2011] for data of all spectral bands, except the sixth (thermal) one; or unsupervised image classification which Chirico and Malpeli [2012] applied to near-infrared optical imagery and RADAR data verified against a *GeoEye-1* control dataset for identification of hydrography features.

The key problem in assessing the accuracy of lake areas is the choice of control water bodies of dif-

ferent sizes. Maps are not very useful in this respect because their creation takes a long time and the mapped surface areas of water bodies are average values. A better way is to use reference lakes identified in aerial photographs or in images of ultrahigh (meter and submeter) resolution collected by *Ikonos*, *WorldView-1*, *WorldView-2*, *QuickBird*, or *GeoEye-1* satellites [Frohn et al., 2005; Elsakov and Marushchak, 2011; Chirico and Malpeli, 2012; Bryksina and Polishchuk, 2013]. Permafrost hydrography, and lake surface areas, are highly variable in the warm season [Baranov et al., 2012] strongly depending on weather (amount of moisture) [Kravtsova and Tarasenko, 2011]. Therefore, the compared higher- and lower-resolution images should be acquired on the closest possible dates.

ACCURACY OF LAKE AREA ESTIMATES FROM *GeoEye-1* DATA

The accuracy of *GeoEye-1* area estimates were assessed for 170 water bodies with a total area of ~ 3.9 km² located near the Marre-Sale polar station in the western coast of the Yamal Peninsula (Fig. 1). The study area occupies about 30 km² and abounds in near-surface ground ice [Kritsuk, 2010]. The largest thaw lakes and drained thaw lake basins (locally called *hasyrei*) have round or oval shapes indicating their thermokarst origin. The selected sample contained lakes ranging in surface areas from 69 m² to 1.24 km² (Siurtiav-Malto lake the largest). The analyzed images were acquired by *GeoEye-1* on

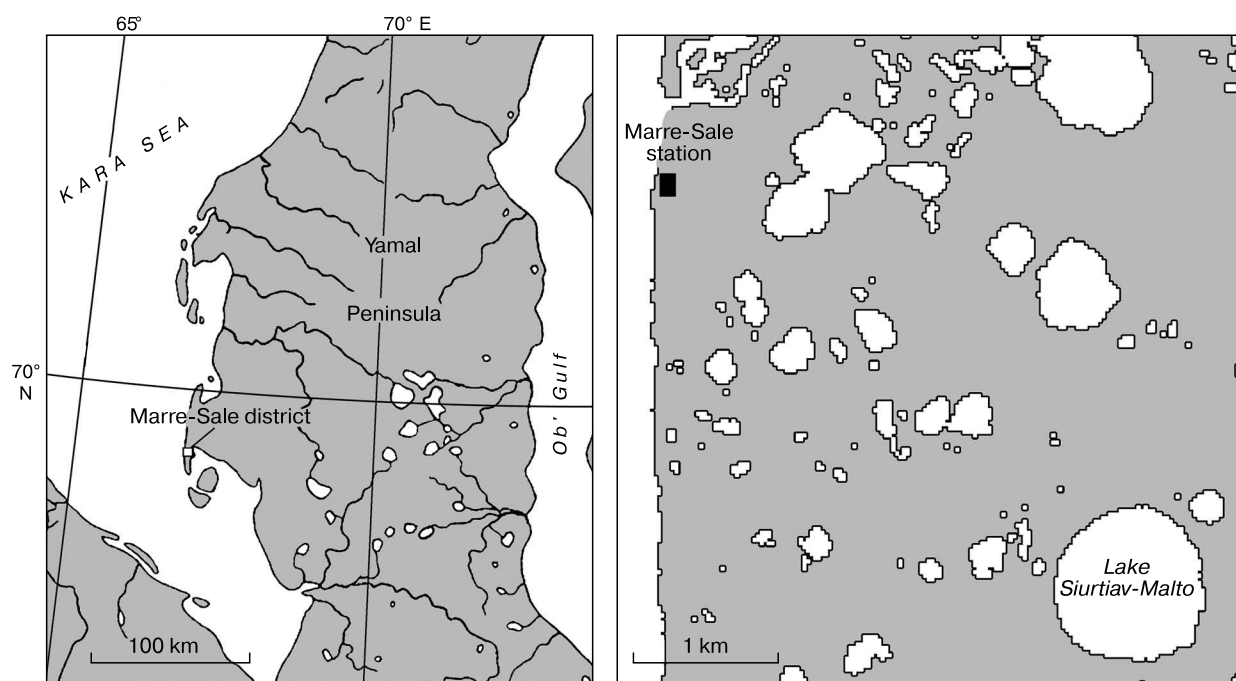


Fig. 1. Location map of study area.

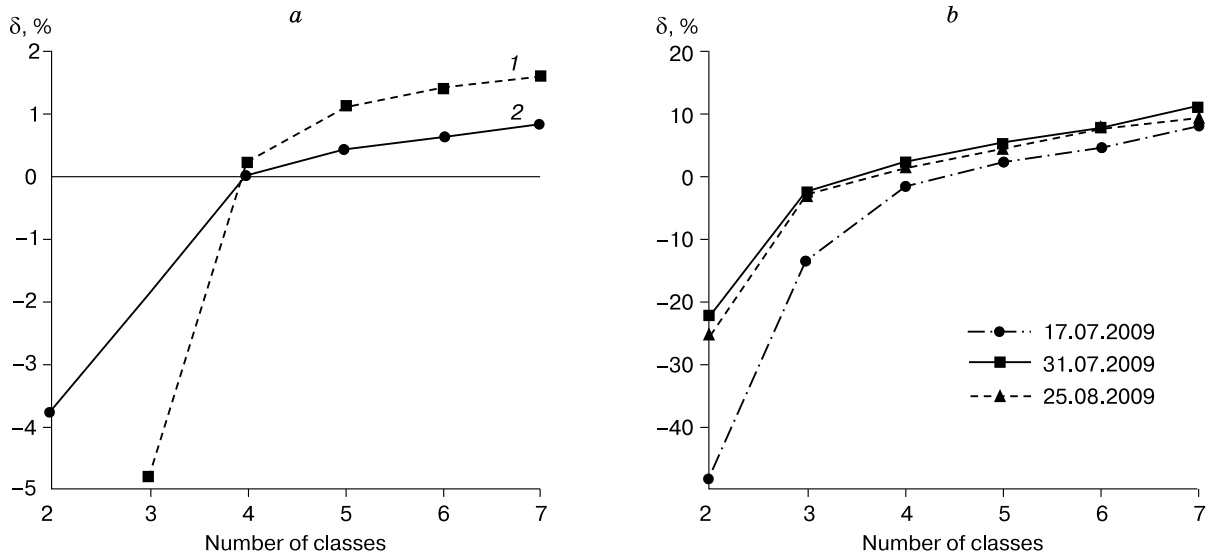


Fig. 2. Relative errors in lake areas (δ) estimated from *GeoEye-1* (a) and *Landsat 5* (b) data vs. number of classes.

1 – Lake Siurtiav-Malto; 2 – all water bodies.

22.07.2009, to a spatial resolution of 0.5 m in the panchromatic (0.45–0.90 μm) band and 2 m in the multispectral (MS) bands (0.45–0.52, 0.52–0.60, 0.625–0.795, and 0.76–0.90 μm). The data were processed using the ENVI 4.8 software. The accuracy of *GeoEye-1* and *Landsat 5* multispectral area estimates was checked against the areas of control lakes classified manually in the panchromatic *GeoEye-1* image. The relative and absolute errors were

$$\delta = \frac{S_r - S}{S_r} \cdot 100\% \text{ and } |\delta| = \frac{|S_r - S|}{S_r} \cdot 100\%,$$

where S_r is the control lake surface area used as reference, and S is this area according to *GeoEye-1* or *Landsat 5* data. The magnitude of relative error is assumed to be the basic accuracy indicator.

Given that the panchromatic and multispectral *GeoEye-1* scenes were collected synchronously, the errors in lake areas derived from multispectral data can result uniquely from the properties of the lakes and the processing techniques. We tried different classification algorithms available in ENVI 4.8 to identify lakes in the multispectral *GeoEye-1* images. Adaptive classification was less accurate, possibly because the training samples failed to cover all spectral variations required to discern the numerous shallow (<2 m) lakes, some with high water turbidity. On the other hand, unsupervised classification (*IsoData* and *K-Means* algorithms) gave more precise and almost identical results.

As mentioned above, near-infrared bands are most often used for classification of water bodies. In our case, four *GeoEye-1* bands provided almost the

same classification quality as the single near-infrared band (0.76–0.90 μm), but the accuracy of the latter was slightly lower at any number of classes. The dependence of accuracy on the number of classes (plotted in Fig. 2, a for the total of lake areas and separately for Lake Siurtiav-Malto) shows the least error at division into four classes. Therefore, the *IsoData* unsupervised classification with four classes was selected to map lakes from the four-band multispectral *GeoEye-1* data. That was the best possible choice, which is evident from the pattern of relative errors as a function of lake area nearly symmetrical about zero (Fig. 3, a).

Lake area errors were correlated with the respective surface areas for seven size groups of lakes. The largest lake of Siurtiav-Malto (Fig. 1) was left beyond any group, and the uncertainty in its area was used as reference to check the quality of estimates from the empirical relationship. The average areas in the lake size groups (Table 1) were estimated from control lakes identified in the panchromatic *GeoEye-1* image.

Empirical relationships were obtained for average $|\delta_{\text{av}}|$ and maximum $|\delta_{\text{max}}|$ errors vs. average areas (S_{av}) in lake size groups (Fig. 3, b). The multispectral *GeoEye-1*-based area of control lake Siurtiav-Malto (1.24 km²) was 99.6 % accurate, while the calculations according to the empirical relationships were less accurate: $|\delta_{\text{av}}| = 0.059$ and $|\delta_{\text{max}}| = 0.25$ %. The larger latter values may be due to the fact that, unlike the round control lake with a smooth shoreline, the other lakes have less regular shapes and curved contours. In this case, $|\delta_{\text{av}}|$ represents the area accuracy

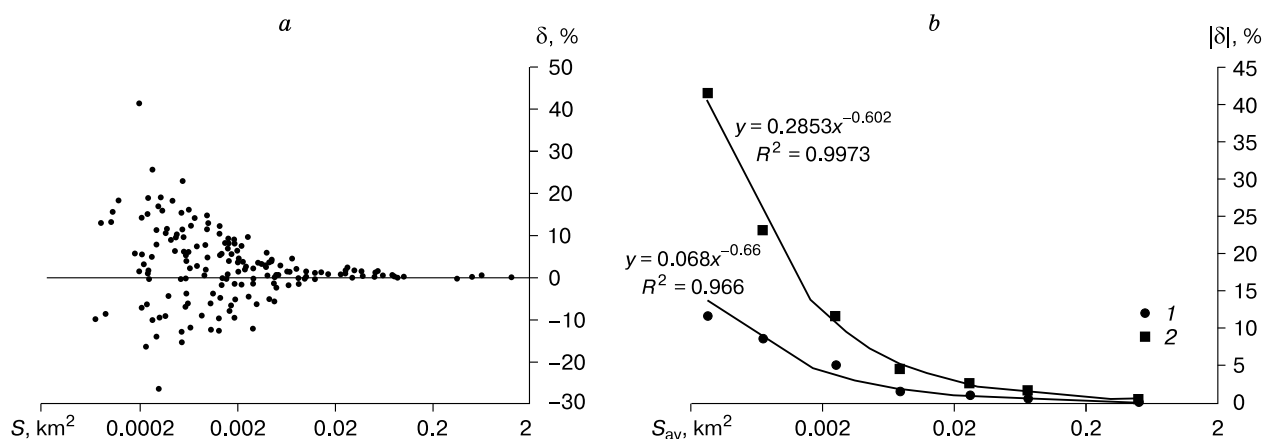


Fig. 3. Relative errors in lake areas (δ) vs. lake sizes S (a) and empirical relationships of average $|\delta_{av}|$ (1) and maximum $|\delta_{max}|$ (2) errors vs. average areas of lakes (S_{av}) within size groups (b) (from a multispectral *GeoEye-1* image).

Table 1. Initial parameters of lake size groups and errors in lake areas from *GeoEye-1* data

Group	S , km ²	n	S_{av} , km ²	$ \delta_{av} $, %	$ \delta_{max} $, %	Rms error $ \delta $, %
1	0.0001–0.0005	41	0.0003	11.69	41.36	7.80
2	0.0005–0.001	30	0.0007	8.53	23.17	5.65
3	0.001–0.005	61	0.0025	4.96	11.64	3.39
4	0.005–0.01	12	0.0076	1.49	4.60	1.28
5	0.01–0.05	14	0.0263	0.99	2.43	0.71
6	0.05–0.1	8	0.0706	0.55	1.45	0.50
7	0.1–1.0	3	0.4906	0.16	0.46	0.25

Note. n is the number of water bodies in a group.

for lakes of the most frequent geometry while $|\delta_{max}|$ refers mainly to tortuous lakes. The measured and calculated $|\delta_{av}|$ errors for Lake Siurtiav-Malto are of the same order of magnitude anyway, i.e., the obtained empirical relationship is applicable to assess the accuracy of lake areas identified by unsupervised classification of multispectral *GeoEye-1* images.

ACCURACY OF LAKE AREA ESTIMATES FROM *Landsat 5* DATA

The accuracy of *Landsat 5* lake area estimates was assessed using three scenes acquired on 17.07.2009, 31.07.2009 and 25.08.2009, to a spatial resolution of 30 m, in 4, 5 and 7 bands of long (0.76–0.90 μm) and medium (1.55–1.75, 2.08–2.35 μm) wavelengths; the classification was with the *IsoData* algorithm. As noted above, the estimates are reliable if the control and target images are acquired on closest possible dates. The date of *Landsat 5* acquisition closest to that of the control *GeoEye-1* image (22.07.2009) was 17.07.2009. However, a later date of 31.07.2009 was preferred because lake areas change much by seasonal inundation earlier in summer [Baranov et al., 2012] but stabilize by the end of July.

That was a good choice: the data of 31.07.2009 and 25.08.2009 gave similar results. The assessment was verified against data for 61 out of 170 control lakes varying from 1270 m² to 1.24 km² (Siurtiav-Malto Lake), with a total surface area of 3.77 km². Again, the total lake area was the most accurate in the case of four classes in the classification of *Landsat 5* multispectral images (Fig. 2, b).

Most of errors in the areas of individual lakes classified according to *Landsat 5* data of 31.07.2009 are positive (see the distribution in Fig. 4, a), which indicates that the *Landsat 5*-based total lake area is underestimated relative to the control (*GeoEye-1*) dataset, possibly because of the mismatch in acquisition dates. On the other hand, the smaller number of classes leads to overestimation of the total lake area and worse accuracy (Fig. 2, b). As in the previous case, all lakes were divided into six size groups (Table 2) for obtaining empirical lake area dependences of errors ($|\delta_{av}|$ and $|\delta_{max}|$).

The average and maximum errors in lake areas estimated from the empirical relationships vs. average area (S_{av}) in size groups (Fig. 4, b) are $|\delta_{av}| = 0.91$ and $|\delta_{max}| = 1.31$ %, for lakes commensurate with the con-

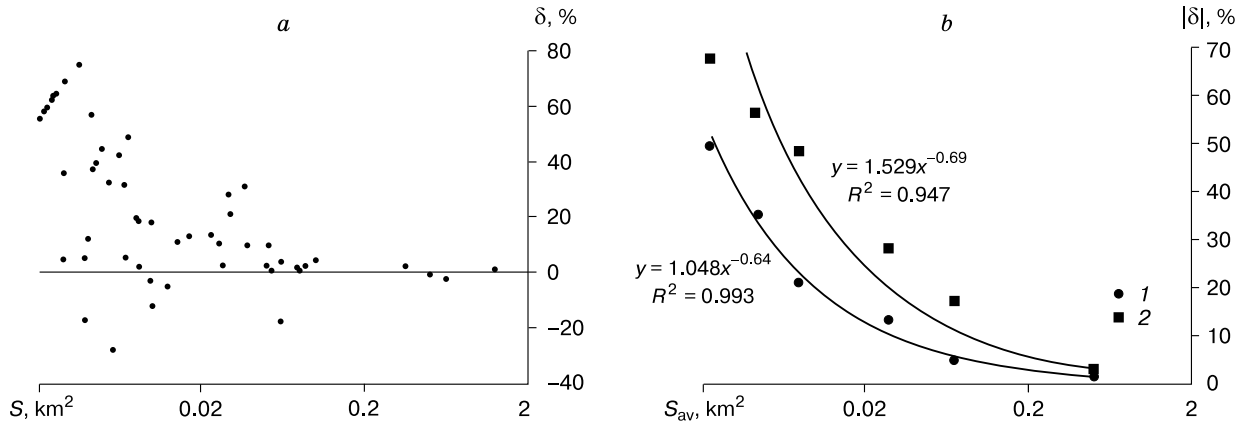


Fig. 4. Relative errors in lake areas (δ) vs. lake sizes S (a) and empirical relationships of average $|\delta_{av}|$ (1) and maximum $|\delta_{max}|$ (2) errors vs. average areas of lakes (S_{av}) within size groups (b) (from a multispectral *Landsat 5* image).

Table 2. Initial parameters of lake size groups and errors in lake areas from *Landsat 5* data

Group	S , km ²	n	S_{av} , km ²	$ \delta_{av} $, %	$ \delta_{max} $, %	Rms error $ \delta $, %
1	0.001–0.003	17	0.0022	49.86	68.47	18.58
2	0.003–0.005	10	0.0042	35.52	57.07	20.92
3	0.005–0.01	11	0.0077	21.31	48.85	15.82
4	0.01–0.05	11	0.0273	13.50	28.18	9.55
5	0.05–0.1	8	0.0706	5.15	17.43	5.77
6	0.1–1.0	3	0.4905	1.61	2.16	0.87

trol lake of Siurtiav-Malto. The calculated average error is the same as the measured value for the control lake (0.91 %), i.e., the obtained empirical relationships are valid for assessing the accuracy of lake areas from *Landsat 5* data, with the selected classification.

The empirical equations (Figs. 3, b; 4, b) were used to constrain the correlations of $|\delta_{av}|$ and $|\delta_{max}|$ with the lake areas and with the spatial resolution. Lake areas estimated from multispectral *GeoEye-1* data can be 99 % or more accurate ($|\delta_{max}| < 1$ %) if the target lake area is $3.07 \cdot 10^4$ times S_G ; the respective ratio for *Landsat 5* is $2.64 \cdot 10^3 S_L$ (Table 3), where S_G and S_L are land areas corresponding to a pixel of *GeoEye-1* and *Landsat 5* images, respectively. Therefore, the lake area accuracy better than 99 % is possible for the lakes that are at least four or five orders of magnitude larger than the pixel area.

The ratios of average errors in *Landsat 5* and *GeoEye-1* estimates ($|\delta_{av,L}|$ and $|\delta_{av,G}|$) were compared with the respective resolution ratios (Table 4). The ratios of errors $|\delta_{av,L}|/|\delta_{av,G}|$ approached $\sqrt{S_L/S_G} = 15$ at different lake areas. In other words, the error ratio is close to the ratio of pixel sides. Therefore, the resolution of satellite images may be used to check the validity of error vs. lake area empirical relationships.

Table 3. Correlation of lake area accuracy with lake size and spatial resolution of *GeoEye-1* and *Landsat 5* data

$ \delta_{av} $, %	Ratio of lake area to land area corresponding to one pixel	
	<i>GeoEye-1</i> ($S_G = 4 \text{ m}^2$)	<i>Landsat 5</i> ($S_L = 900 \text{ m}^2$)
10.0	$1.20 \cdot 10^2$	$0.33 \cdot 10^2$
1.0	$5.75 \cdot 10^3$	$1.15 \cdot 10^3$
0.1	$2.75 \cdot 10^5$	$4.00 \cdot 10^4$
$ \delta_{max} $, %		
10.0	$6.87 \cdot 10^2$	$0.86 \cdot 10^2$
1.0	$3.07 \cdot 10^4$	$2.64 \cdot 10^3$
0.1	$1.37 \cdot 10^6$	$8.17 \cdot 10^4$

Table 4. Accuracy of lake areas estimated from *Landsat 5* and *GeoEye-1* data, compared

S , km ²	$ \delta_{av,L} $, %	$ \delta_{av,G} $, %	$ \delta_{av,L} / \delta_{av,G} $
10.0	0.24	0.0148	16.21
1.0	1.05	0.0680	15.41
0.1	4.57	0.3100	14.74

Note. δ_{av} is mean relative error; $\delta_{av,L}$ is error for *Landsat 5*; $\delta_{av,G}$ is error for *GeoEye-1*.

DISCUSSION

The above results can be compared in terms of accuracy with published evidence of lake areas estimated from multispectral *Landsat 5* [Bryksina and Polishchuk, 2013] and Advanced Land Observing Satellite (ALOS) Phased Array type L-band Synthetic Aperture RADAR (PALSAR) [Chirico and Malpeli, 2012] data. The cited data were used to estimate average relative errors for lakes with the areas 10.0, 1.0, and 0.1 km² (Table 5). The errors in lake areas obtained from *Landsat 5* images in this study (Marre-Sale site) and reported in [Bryksina and Polishchuk, 2013] are quite similar for lake areas of 1.0 km² but differ a little more for 10.0 km² and 0.1 km². The latter difference may be due to a large misfit of the acquisition dates between the *Landsat 5* (17.07.2006, 21.07.2008) and control *QuickBird* (15.08.2006, 02.09.2008) images [Bryksina and Polishchuk, 2013]. Furthermore, it is difficult to compare the results and analyze the factors of accuracy because [Bryksina and Polishchuk, 2013] provided no data processing details. Nevertheless, the general similarity of the results shows that the obtained empirical relationships are applicable to assess the accuracy (average relative error) of lake areas based on *Landsat* imagery.

The lake areas estimated by ALOS (PALSAR) remote sensing [Chirico and Malpeli, 2012] are notably less accurate in spite of the 12.7 m radar resolution, almost three times higher than in *Landsat 5*. The worse accuracy may be also due to a large acquisition time misfit of the target and control datasets (the ALOS and *GeoEye-1* images were collected on 12.06.2010 and 11.07.2009, respectively). Otherwise, the radar-based areas might be less accurate because the lakes in the Bahamas are more tortuous than the round thaw lakes in Yamal. This explanation, however, contradicts the 98.4 % accurate (no worse than $|\delta_{\max}| = 1.6\%$) *Landsat 5*-based areas of ≤ 1 km² tortuous lakes according to the obtained empirical relationship (Fig. 4, b), which is three times better than the accuracy provided by the ALOS (PALSAR) data ($|\delta_{\text{av}}| = 4.45\%$, Table 5). More likely, the lake areas estimated by the higher-resolution ALOS (PALSAR) sensing are less accurate due to off-nadir acquisition.

Obviously, any reports of remote sensing lake area estimates should provide information on process-

ing algorithms, as well as the accuracy of data and the methods of its assessment. The accuracy of lake areas identified from satellite multispectral optical imagery depends on the number of classes in the classification. Therefore, high-quality lake area estimates require the appropriate number of classes and classification algorithms. According to the error vs. lake area empirical relationships obtained in this study, the errors correspond to threshold significant changes in the lake areas, which are detectable from satellite images shot at different times and are applicable as indicators of natural and anthropogenic processes in permafrost.

CONCLUSIONS

1. Assessment with reference to examples of permafrost thaw lakes in the western coast of the Yamal Peninsula (Marre-Sale district) shows that the accuracy of lake areas estimated by satellite remote sensing depends on the number of land cover classes used in data classification; the estimates from *GeoEye-1* and *Landsat 5* multiband data were the most accurate in the case of unsupervised classification with four classes.

2. Empirical relationships have been obtained for lake size dependence of average and maximum relative errors in the areas of lakes identified from satellite images of different resolutions.

3. The lake area accuracy correlates with spatial resolution of spaceborne data. Namely, the lake areas from *Landsat 5* and *GeoEye-1* data can be accurate to 99 % or better if the target lakes are at least four or five orders of magnitude larger than the land area corresponding to one pixel.

4. The resolution of satellite images may be used to check the validity of error vs. lake area empirical relationships, because the ratio of lake area errors estimated from images of different resolutions approaches the ratio of the respective pixel sides.

The study was carried out as part of Project 2.3.2 of Program 27 of the RAS Presidium "Remote Sensing for Monitoring of Environment and Engineering Hazards in Arctic and Subarctic Development Areas".

References

- Baranov, Yu.B., Kiselevskaya, K.I., Kozhina, L.Yu., 2012. An experience of using radar remote sensing for hydrology. *Geomatika*, No. 4, 76–81.
- Bryksina, N.A., Polishchuk, Yu.M., 2009. Seasonal changes in surface areas of thaw lakes in West Siberian permafrost: evidence from ERS-2 satellite imagery. *Issled. Zemli iz Kosmosa*, No. 3, 90–93.
- Bryksina, N.A., Polishchuk, Yu.M., 2013. Accuracy of satellite remote sensing estimation of lake areas. *Geoinformatika*, No. 1, 64–68.
- Chen, M., Rowland, J.C., Wilson, C.J., et al., 2013. The importance of natural variability in lake areas on the detection of

Table 5. Accuracy of lake areas estimated from *Landsat 5* and ALOS (PALSAR) radar data, compared

S, km ²	Landsat 5* (Marre-Sale)	Landsat 5**	ALOS (PALSAR)***
10.0	0.24	0.55	2.33
1.0	1.05	1.40	4.45
0.1	4.57	3.53	8.48

* this study; ** after [Bryksina and Polishchuk, 2013]; *** after [Chirico and Malpeli, 2012].

- permafrost degradation: A case study in the Yukon Flats, Alaska. *Permafrost and Periglacial Processes* 24 (3), 224–240.
- Chirico, P.G., Malpeli, K.C., 2012. Inland and coastal hydrographic feature identification in the Bahamas using RADAR data and raster processing in a GIS. *J. Geography and Geol.* 4 (3), 29–42.
- Dneprovskaya, V.P., Bryksina, N.A., Polishchuk, Yu.M., 2009. Changes of thermokarst in discontinuous permafrost in West Siberia: evidence from satellite images. *Issled. Zemli iz Kosmosa*, No. 4, 88–96.
- Elsakov, V.V., Marushchak, I.O., 2011. Inter-annual variability of thaw lakes in northeastern European Russia. *Issled. Zemli iz Kosmosa*, No. 5, 45–57.
- Frohn, R.C., Hinkel, K.M., Eisner, W.R., 2005. Satellite remote sensing classification of thaw lakes and drained thaw lake basins on the North Slope of Alaska. *Remote Sensing of Environ.* 97 (1), 116–126.
- Kondratiev, K.Ya., Shumakov, F.T., 1990. Hydrographic monitoring by visible and near-infrared satellite remote sensing: Physical background. *Issled. Zemli iz Kosmosa*, No. 6, 44–48.
- Kravtsova, V.I., Bystrova, A.G., 2009. Changes in thermokarst lake size in different regions of Russia for the last 30 years. *Kriosfera Zemli XIII* (2), 16–26.
- Kravtsova, V.I., Tarasenko, T.V., 2011. The dynamics of thermokarst lakes under climate changes since 1950, Central Yakutia. *Kriosfera Zemli XV* (3), 31–42.
- Kritsuk, L.N., 2010. *Ground Ice in West Siberia*. Nauchniy Mir, Moscow, 352 pp. (in Russian)

Received January 23, 2014